Journal of Mathematics Research; Vol. 12, No. 5; October 2020
ISSN 1916-9795 E-ISSN 1916-9809
Published by Canadian Center of Science and Education

Application of a Rank-One Perturbation to Pendulum Systems

Traoré. G. Y. Arouna[1], M. Dosso[1], J.-C. Koua Brou[1]

[1] Université Félix Houphouët-Boigny de cocody-Abidjan. Laboratoire de Mathématiques Appliquées. UFR Mathématiques et Informatique, 22 BP 582 Abidjan 22, Côte d'Ivoire

Correspondence: M. Dosso, Université Félix Houphouët-Boigny de cocody-Abidjan. Laboratoire de Mathématiques Appliquées. UFR Mathématiques et Informatique, 22 BP 582 Abidjan 22, Côte d'Ivoire

Received: July 20, 2020 Accepted: August 25, 2020 Online Published: September 15, 2020

doi:10.5539/jmr.v12n5p47 URL: https://doi.org/10.5539/jmr.v12n5p47

Abstract

From a perturbation theory proposed by Mehl, et al., a study of the rank-one perturbation of the problems governed by pendulum systems is presented. Thus, a study of motion of the simple pendulum, double and triple pendulums with oscillating support, not coupled as coupled by a spring and double pendulum with fixed support is proposed. Finally (strong) stability and instability zones are calculated for each studied system.

Keywords: Hill systems, Hamiltonian systems, fundamental solutions, monodromic matrices, rank-one perturbation, (strong)stability

1. Introduction

Consider the following Hill's equation $\frac{d^2x_i}{dt^2} + \varphi_i(t)x_i = 0,\ i = 1, ..., N,$ where φ_i are periodic functions and $N \geq 1$. This type of equation is part of an important class of differential equations (see (Hoffmann & Stroobant, 2007), (Hsu, 1961) and (Yakubovich & Starzhinskii, 1975)). Hill's equations appear in several scientific fields such as: physics, mechanics and chemistry. In these fields, these types of equations are used more officially in the study of the stability of certain real phenomena such as the motion of a pendulum (see in (Hsu, 1961) and (Lalanne, Berthier, & Der Hagopian, 1984)), the motion of an ion through a quadrupole analyzer (see (Hoffmann & Stroobant, 2007)), the vibratory motion of an elliptical membrane (see in (Mathieu, 1868)) and so on. These equations can be in the following Hamiltonian form (see for example (Dosso, 2006) and (Dosso & Coulibaly, 2014)):

$$J\frac{dX(t)}{dt} = H(t)X(t), \quad X(0) = I_{2N} \tag{1}$$

where $t \longmapsto H(t)$ is a piecewise continues and periodic matrix function, J is an invertible and skew-symmetric matrix and I_{2N} the identity matrix of order $2N$.

Using the following change of variables:

$$X(t) = \begin{bmatrix} x \\ \frac{dx}{dt} \end{bmatrix},\ J = \begin{bmatrix} 0_N & -I_N \\ I_N & 0_N \end{bmatrix} \text{ and } H(t) = \begin{bmatrix} P(t) & 0_N \\ 0_N & I_N \end{bmatrix}, \tag{2}$$

where

$$x(t) = Vec((x_k)_{1\leq k\leq 2N}), \qquad P(t) = diag\left((\varphi_i(t))_{1\leq i\leq N}\right) \tag{3}$$

with $\varphi_i(t)$ periodic functions. The notations I_N, $Vec((x_k)_{1\leq k\leq 2N})$ and $diag\left((\varphi_i(t))_{1\leq i\leq N}\right)$ given in (2) and (3) denote respectively the identity matrix of order N, the column vector of coefficients $((x_k)_{1\leq k\leq 2N})$ and the diagonal matrix with $(\varphi_i(t))_{1\leq i\leq N}$ on the main diagonal. The fundamental solutions $(X(t))_{t\in\mathbb{R}}$ of (1) are J-symplectic (i.e $X^T(t)JX(t) = J,\ \forall\ t \in \mathbb{R}$) and the one obtained at period P is called the monodronic matrix of the Hamiltonian system (1) (see in (Dosso, 2006), (Dosso & Coulibaly, 2014) and (Yakubovich & Starzhinskii, 1975)).

Let $W \equiv X(P)$ be the monodronic matrix of system (1). This matrix plays a very important role in the strong stability study of differential systems because its strong stability is equivalent to that of system (1) (see (Arouna, Dosso, & Koua Brou, 2018),(Dosso, 2006), (Dosso & Coulibaly, 2014) and (Yakubovich & Starzhinskii, 1975)). Thus, it suffices to know the nature of stability of this matrix to deduce that of system (1). Considering the spectrum of the monodronic matrix W, we have the following classification given by Godunov and Sadkane in (Godunov & Sadkane, 2001) and (Godunov & Sadkane, 2006).

Definition 1 *Let λ be a semi-simple eigenvalue of a symplectic matrix W on the unit circle. We say that λ is of the red (respectively green) color or in short r-eigenvalue (respectively g-eigenvalue) if $(S_0x,\ x) > 0$ (respectively $(S_0x,\ x) < 0$) on the eigenspace associated with λ, where $S_0 = \frac{1}{2}\left[(JW) + (JW)^T\right]$. If $(S_0x,\ x) = 0$, we say that λ is of mixed color.*

In definition 1, the notation (., .) denoted an inner scalar product.

From this classification, the following proposition gives us the conditions of the strong stability of the monodromy of a symplectic matrix W.

Proposition 1 *W is strongly stable if and only if:*

1) *all its eigenvalues are on the unit circle;*

2) *its eigenvalues are either red color or either green color;*

3) *the quantity*

$$\delta_S = min\{|e^{i\theta_l} - e^{i\theta_j}| : e^{i\theta_l}, e^{i\theta_j} \ are\ r\text{-}\ and\ g\text{-}eigenvalues\ of\ W\}$$

should not be close to zero.

From this proposition, we recall the following theorem deduce from (Arouna, Dosso, & Koua Brou, 2018), (Dosso, 2006), (Dosso, Arouna, & Koua Brou, 2018), (Dosso & Sadkane, 2013), (Dosso & Coulibaly, 2014) and (Yakubovich & Starzhinskii, 1975).

Theorem 1 *The system (1) is strongly stable if and only if one of the following conditions is verified*

1) *the monodromy matrix W of system (1) is strongly stable.*

2) *the sequence of matrix average $(S^{(n)})_{n\geq 0}$ definied by*

$$S^{(n)} = \frac{1}{2^n}\sum_{j=1}^{2^n}(W^T)^{j-1}(W)^{j-1}$$

converges to a positive definie symmetric constant matrix $S^{(\infty)}$ and the quantity

$$\delta_S = min\{|e^{i\theta_l} - e^{i\theta_j}| : e^{i\theta_l}, e^{i\theta_j} \ are\ r\text{-}\ and\ g\text{-}eigenvalues\ of\ W\}$$

is not close to zero.

3) *there exists $\varepsilon > 0$ such that any Hamiltonian system with P-periodic coefficients of the form*

$$J\frac{dX(t)}{dt} = \widetilde{H}(t)X(t), \tag{4}$$

verifying $\|H - \widetilde{H}\| \equiv \int_0^P |H(t) - \widetilde{H}(t)|dt < \varepsilon$ is stable.

In this paper, we are interested to the application of the perturbation theory proposed in (Dosso, Arouna, & Koua Brou, 2018) to pendulum systems. Thus, we recall the definition of the rank-one perturbation of a Hamiltonian system given in (Dosso, Arouna, & Koua Brou, 2018):

Definition 2 *We call rank-one perturbation of Hamiltonian system with periodic coefficients (1) any differential system of the form*

$$J\frac{d\widetilde{X}(t)}{dt} = (I - uu^TJ)^TH(t)(I - uu^TJ)\widetilde{X}(t), \quad \widetilde{X}(0) = I_{2N} + uu^TJ \tag{5}$$

where $u \in \mathbb{R}^{2N}$ is a non-zero random vector. From this definition and results of (Dosso, Arouna, & Koua Brou, 2018), we give as a consequence of the strong stability of (1) on its rank-one perturbation as follows.

Proposition 2 *If system (1) is strongly stable, then there exists $\varepsilon > 0$ such that for any vector $u \in \mathbb{R}^{2N}$ verifying $\|uu^TJW\| < \varepsilon$, we have $\widetilde{X}(P) = (I + uu^TJ)W$ is stable, where $W \equiv X(P)$.*

The purpose of this present paper is to analyze the (strong) stability of some everyday problems governed by Hamiltonian systems with periodic coefficients using the perturbation theory introduced in (Dosso, Arouna, & Koua Brou, 2018). The paper is organized as follows: in section 2, we study the stability of the motion of a simple pendulum with oscillating support. The third and fourth sections are respectively dedicated to the study of the stability of the motion of the double and triple pendulum with oscillating supports. In each of these sections, our study is organized in two parts. In the first part, we study the case where the double and triple pendulums are not coupled and in the second part, we study the case where these pendulums are coupled by a spring. Finally, in the last section, we are interested in the study of the (strong) stability of the motion of a double pendulum with fixed supports.

Throughout this paper, the symbol $\|.\|$ denotes the Euclidean norm of matrices or vectors. In the present figures, the zones in red, blue and white color denote respectively the zones of instability, stability and strong stability of the rank-one perturbation of (1).

2. Simple Pendulum With Oscillating Support

Consider the following simple pendulum (see Figure1) whose support is subjected to an oscillating motion $f(t)$ defined by $f(t) = \alpha\cos(\Omega t)$ in (Hsu, 1961).

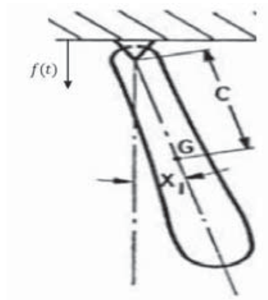

Figure 1. Model of the simple pendulum with oscillating support

According to (Hsu, 1961), the equation of motion of the simple pendulum is governed by

$$\frac{d^2x}{dt^2} + \frac{cg}{k_0^2}\left(1 + \frac{\alpha\Omega^2}{g}\cos(\Omega t)\right)x = 0, \tag{6}$$

where k_0 is the radius of gyration of the pendulum about its point of suspension and c the distance between the point of suspension and the center of the pendulum. This equation can be written as a Mathieu's equation of the form (see (Hsu, 1961))

$$\frac{d^2x}{d\tau^2} + (\delta + \epsilon\cos(\tau))\,x = 0, \tag{7}$$

where

$$\tau = \Omega t,\ \ \epsilon = \frac{c\alpha}{k_0^2} \text{ and } \delta = \frac{cg}{k_0^2\Omega^2}.$$

Using the change of variable given in (2) with $N = 1$, it is easy to see that (7) can be reduce to Hamiltonian form (1), with

$$H(\tau, \delta, \epsilon) = \begin{bmatrix} \delta + \epsilon\cos(\tau) & 0 \\ 0 & 1 \end{bmatrix} \text{ and } J = \begin{bmatrix} 0 & -1 \\ 1 & 0 \end{bmatrix}.$$

To analyze the (strong) stability of the motion of the pendulum, we perturb the solution $X(\tau, \delta, \epsilon)$ of (1) by the following matrix of rank one:

$$E_a(\tau, \delta, \epsilon) = u_a u_a^T JX(\tau, \delta, \epsilon),$$

where $u_a = \begin{pmatrix} a \\ 0 \end{pmatrix}$ and $a \in [0,\ 1[$. Then the perturb motion of the pendulum is described by:

$$\widetilde{X}_a(\tau, \delta, \epsilon) = \left(I + u_a u_a^T J\right)X(\tau, \delta, \epsilon).$$

According to (Dosso, Arouna, & Koua Brou, 2018), the equation of the pendulum's motion then can be written as:

$$J\frac{d\widetilde{X}_a(\tau, \delta, \epsilon)}{d\tau} = \underbrace{(I - u_a u_a^T J)^T H(\tau, \delta, \epsilon)(I - u_a u_a^T J)}_{\widetilde{H}(\tau,\delta,\epsilon,a)}\widetilde{X}_a(\tau, \delta, \epsilon), \quad \widetilde{X}_a(0, \delta, \epsilon) = I_2 + u_a u_a^T J \tag{8}$$

The spectral portrait and the (strong) stability zone of the matrix solution $\widetilde{X}_a(\tau, \delta, \epsilon)$ of equation (8) are respectively plotted in Figure 2 and Figure 3 for $\tau \in [0,\ 2\pi]$ and $(\delta, \epsilon) \in \{(1, 0.8)\,,\ (1.93, 1.93)\}$, with $a \in \{0,\ 0.35\}$.

In Figure 2, we notice a small change in the spectral portrait of $\widetilde{X}_a(\tau, \delta, \epsilon)$ for $\delta = 1$ and $\epsilon = 0.8$ whereas for $\delta = 1.93$ and $\epsilon = 1.93$, we don't observe any change in its spectral portrait in presence of this rank-one perturbation.

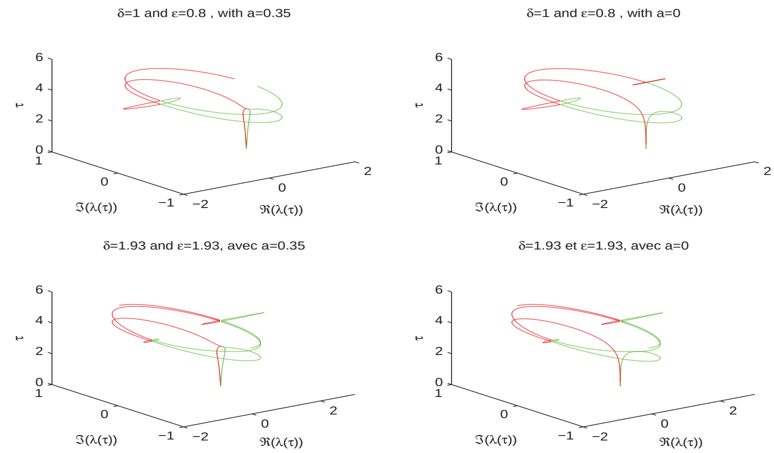

Figure 2. Spectral portrait of $\tau \mapsto \widetilde{X}_a(\tau, \delta, \epsilon)$ for $\tau \in [0,\ 2\pi]$ and $(\delta, \epsilon) \in \{(1, 0.8)\,,\ (1.93,\ 1.93)\}$, with $a \in \{0,\ 0.35\}$

In Figure 3, we observe that the stable region of $\widetilde{X}_a(\tau, \delta, \epsilon)$ obtained in presence of the rank-one perturbation is smaller than that obtained in absence of this perturbation. In fact, $\|S^{(n_0)}(\tau)\|$ takes much lager values when a is different to zero; and the region where $\delta_S(\tau)$ is represented in green color, is small when a is different to zero.

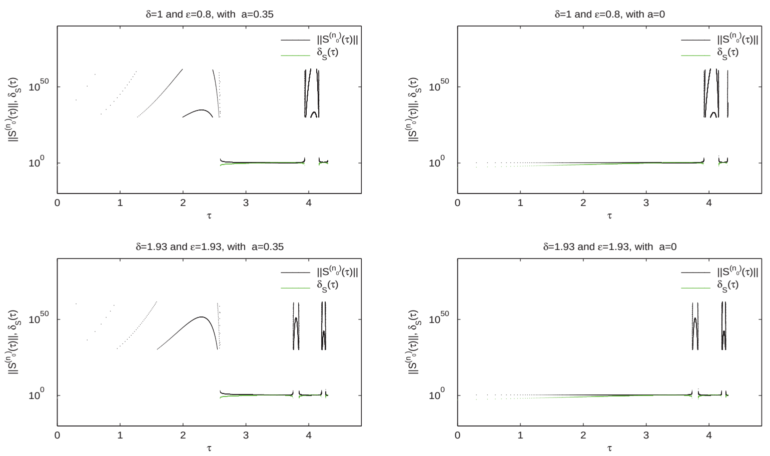

Figure 3. Graph of $\tau \mapsto \|S^{(n_0)}(\tau)\|$ and $\tau \mapsto \|\delta_S(\tau)\|$ for $\tau \in [0,\ 2\pi]$ and $(\delta, \epsilon) \in \{(1, 0.8)\,,\ (1.93,\ 1.93)\}$, with $a \in \{0,\ 0.35\}$

The Figure 4 represents the (strong) stability zone of $\widetilde{X}_a(2\pi, \epsilon, \delta)$ in the plane of parameters $(\delta, \epsilon) \in [0,\ 1.98] \times [0,\ 2]$. In this Figure, we note the presence of two regions: a first zone in red color, representing the unstable zone and a second zone, in white, representing the strong stable zone. In presence of perturbation, we notice a widening of the unstable zone(see Figure on the left). This shows that the perturbation is a factor that increase an instability of the motion of the pendulum.

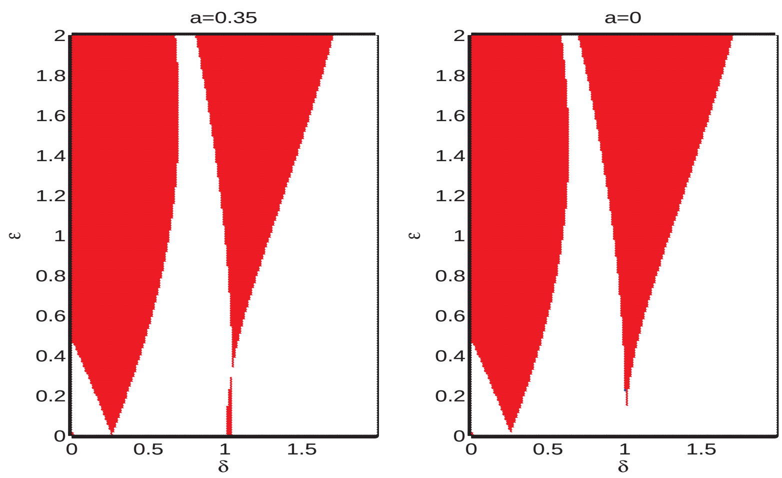

Figure 4. (Strong)stability Zone of $\widetilde{X}_a(2\pi, \delta, \epsilon)$ for $(\delta, \epsilon) \in [0,\ 1.98] \times [0,\ 2]$ and $a \in \{0,\ 0.35\}$

3. Double Pendulum With Oscillating Supports

We consider two identical simple pendulums attached to a support common (see Figures 5 and 9). In this part, we restrict our study to the case where the support of each pendulum is subjected to an oscillatory motion $f(t)$ defined by $f(t) = \alpha\cos(\Omega t)$ (see in (Hsu, 1961)).

3.1 Uncoupled Double Pendulums With Oscillating Supports

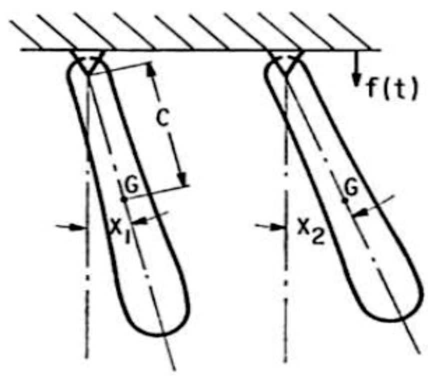

Figure 5. Model of the uncoupled double pendulum with oscillating supports

Since the two pendulums are identical, according to (Hsu, 1961), the equation of the motion of the two pendulums will be the same. Then, the equation of motion is given by:

$$\frac{d^2x_i}{dt^2} + \frac{cg}{k_0^2}\left(1 + \frac{\alpha\Omega^2}{g}\cos(\Omega t)\right)x_i = 0,\ i = 1, 2 \tag{9}$$

where k_0 is the radius of gyration of the pendulum around its point of suspension, and c is the distance between the point of suspension and the center of the pendulum.

Using the change of variable $\tau = \Omega t$ the equation of the system then becomes:

$$\frac{d^2x_i}{d\tau^2} + (\delta + \epsilon\cos(\tau))\,x_i = 0,\ i = 1, 2 \tag{10}$$

where

$$\epsilon = \frac{c\alpha}{k_0^2} \text{ and } \delta = \frac{cg}{k_0^2\Omega^2}.$$

Finally, using the following change of variables defined in (2) with $N = 2$, we obtained system (1) with

$$H(\tau,\ \delta,\ \epsilon) = \begin{pmatrix} P(\tau,\ \delta,\ \epsilon) & 0_2 \\ 0_2 & I_2 \end{pmatrix} \text{ and } P(\tau,\ \delta,\ \epsilon) = diag\left((\alpha_i(\tau))_{1\le i\le 2}\right)$$

In what follows, considering the rank-one perturbation of the fundamental solution $X(\tau, \delta, \epsilon)$ of its corresponding Hamiltonian system by the following matrix of rank one

$$E_a(\tau, \delta,\ \epsilon) = u_a u_a^T JX(\tau, \delta,\ \epsilon), \tag{11}$$

where

$$u_a = a\begin{pmatrix} 1 \\ 0 \\ 0 \\ 0 \end{pmatrix} \text{ and } a \in [0,\ 1[.$$

According to (Dosso, Arouna, & Koua Brou, 2018), its rank-one perturbation is

$$\widetilde{X}_a(\tau, \delta,\ \epsilon) = \left(I + u_a u_a^T J\right) X(\tau, \delta,\ \epsilon) \tag{12}$$

and the equation of motion then becomes

$$\begin{cases} J\dfrac{d\widetilde{X}_a(\tau, \delta,\ \epsilon)}{d\tau} &= \underbrace{(I - u_a u_a^T J)^T H(\tau, \delta,\ \epsilon)(I - u_a u_a^T J)}_{\widetilde{H}(\tau,\delta,\ \epsilon,a)} \widetilde{X}_a(\tau, \delta,\ \epsilon), \\ \widetilde{X}_a(0, \delta,\ \epsilon) &= I + u_a u_a^T J \end{cases} \tag{13}$$

The figure below represents the spectral portrait of $\widetilde{X}_a(\tau, \delta,\ \epsilon)$ for $(\delta,\ \epsilon) \in \{(1, 0.8)\,,\ (1.93,\ 1.93)\}$ and $a \in \{0; 0.35\}$, with $\tau \in [0,\ 2\pi]$. In this figure, we note a small change in the spectral portrait of $\widetilde{X}_a(\tau, \delta,\ \epsilon)$, due to the rank-one perturbation.

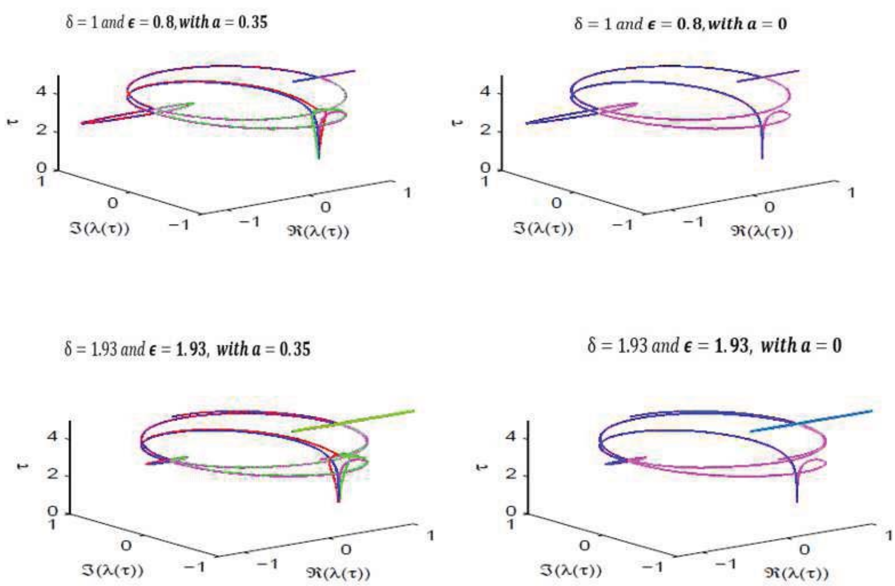

Figure 6. Spectral Portrait of $\tau \mapsto \widetilde{X}_a(\tau, \delta,\ \epsilon)$ for $\tau \in [0,\ 2\pi]$ and $(\delta,\ \epsilon) \in \{(1, 0.8)\,,\ (1.93,\ 1.93)\}$, with $a \in \{0; 0.35\}$

For these parameters, the (strong) stability zone of $\widetilde{X}_a(\tau, \delta,\ \epsilon)$ ($\tau \in [0,\ 2\pi]$) is plotted in Figure 7. This figure shows a coarse widening of the unstable region and a narrowing of the stable region of $\widetilde{X}_a(\tau, \delta,\ \epsilon)$ when the rank-one perturbation is taken into account. In fact, $\|S^{(n_0)}(\tau)\|$ takes much lager values when a is different to zero; and the region where $\delta_S(\tau)$ is represented in green color, is small when a is different to zero.

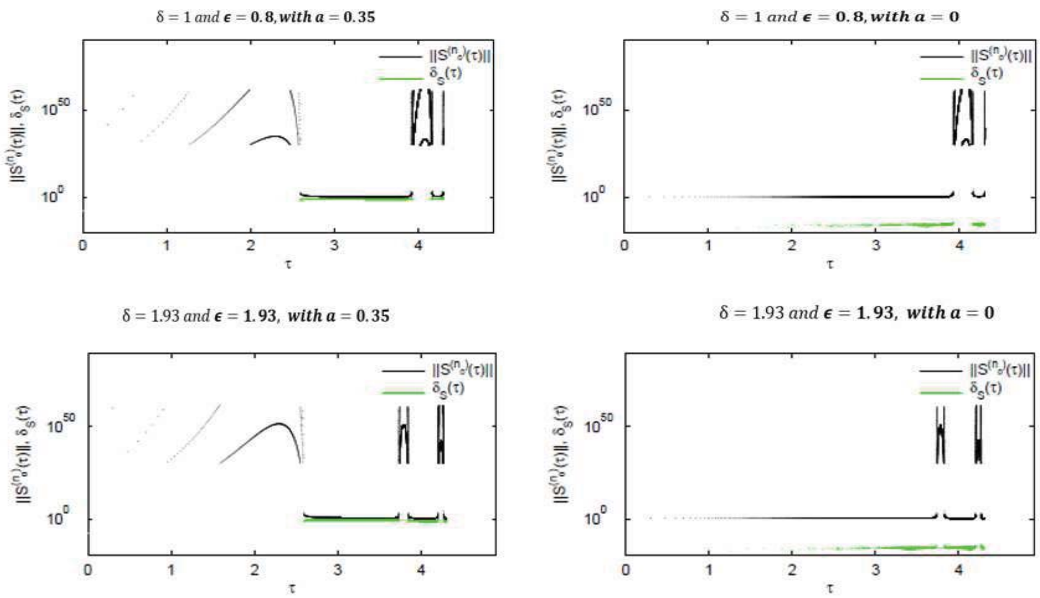

Figure 7. Graphe of $\tau \mapsto \|S^{(n_0)}(\tau)\|$ and $\tau \mapsto \|\delta_S(\tau)\|$ for $\tau \in [0,\ 2\pi]$ and $(\delta, \epsilon) \in \{(1, 0.8)\,,\ (1.93,\ 1.93)\}$, with $a \in \{0; 0.35\}$

In Figure 8, we observe the presence of two regions in the (strong) stability zone: a first zone, in red color, representing the unstable zone and a second zone, in blue, representing the stable zone. When the motion of the two uncoupled pendulums is subjected to the rank-one perturbation, we notice a widening of the unstable zone (see Figure on the left). This shows again that the perturbation is a factor that increase an instability of the motion of the double uncoupled pendulum.

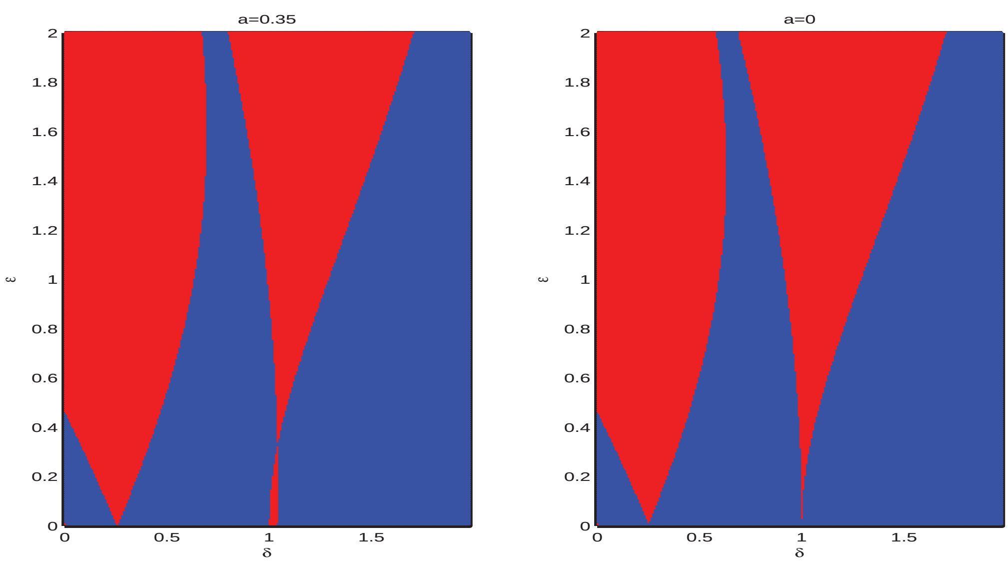

Figure 8. (Strong) stability zone of $\widetilde{X}_a(2\pi, \delta, \epsilon)$ for $(\delta, \epsilon) \in [0,\ 1.98] \times [0,\ 2]$ and $a \in \{0; 0.35\}$

3.2 Coupled Double Pendulums With Oscillating Supports

In this part, the two above simple pendulums are coupled by a spring of constant stiffness k (see Figure 9)

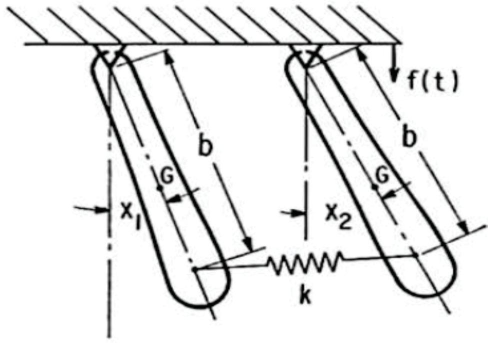

Figure 9. Model of the coupled double pendulum with oscillating supports

According to (Hsu, 1961), the motion of the system is governed by the following differential equation:

$$\frac{d^2x}{dt^2}+\left(B_0+\frac{c\alpha\Omega^2}{k_0^2}\cos(\Omega t)I_2\right)x=0, \tag{14}$$

where

$$x=\begin{pmatrix} x_1 \\ x_2 \end{pmatrix} \text{ and } B_0=\begin{pmatrix} \frac{cg}{k_0^2}+\frac{kb^2}{mk_0^2} & -\frac{kb^2}{mk_0^2} \\ -\frac{kb^2}{mk_0^2} & \frac{cg}{k_0^2}+\frac{kb^2}{mk_0^2} \end{pmatrix},$$

with m the mass of each pendulum and b the distance between the point of suspension and the point of attachment of the coupling spring.

Using successively the following change of variables:

$$z=\begin{pmatrix} z_1 \\ z_2 \end{pmatrix}=\begin{pmatrix} x_1+x_2 \\ x_1-x_2 \end{pmatrix} \text{ and } \tau=\Omega t,$$

the equation of motion of the system then becomes (see for example in (Hsu, 1961)):

$$\frac{d^2z_i}{d\tau^2}+(\delta_i+\epsilon_i\cos(\tau))\,z_i=0,\ i=1,2 \tag{15}$$

where

$$\delta_1=\delta=\frac{cg}{k_0^2\Omega^2},\ \epsilon_1=\epsilon=\frac{c\alpha}{k_0^2} \text{ and } \epsilon_2=\epsilon+2e,\ \text{with } e=\frac{kb^2}{mk_0^2\Omega^2}.$$

Finally, using the change of variables given in (2) with $N=2$, the equation of motion of the coupled system becomes an equation of form (1) with

$$H(\tau,\ \delta,\ \epsilon,\ e)=\begin{pmatrix} P(\tau,\ \delta,\ \epsilon,\ e) & 0_2 \\ 0_2 & I_2 \end{pmatrix}$$

and

$$P(\tau,\ \delta,\ \epsilon,\ e)=\begin{pmatrix} \delta+\epsilon\cos(\tau) & 0 \\ 0 & \delta+2e+\epsilon\cos(\tau) \end{pmatrix}.$$

In what follows, considering that the motion $X(\tau,\delta,\epsilon,\ e)$ of the system is subjected to a perturbation of the form

$$E_a(\tau,\delta,\epsilon,\ e)=u_au_a^TJX(\tau,\delta,\epsilon,\ e), \tag{16}$$

where vector

$$u_a = a \begin{pmatrix} 1 \\ 0 \\ 0 \\ 0 \end{pmatrix};$$

the equation of motion takes form (13).

In Figure 10, we plotted the spectral portrait of $\widetilde{X}_a(\tau, \delta, \epsilon, e)$ for $(\delta, \epsilon, e) \in \{(1, 0.8, 0.5), (1.93, 1.93, 0.5)\}$ and $a \in \{0; 0.35\}$, $\forall \tau \in [0, 2\pi]$.

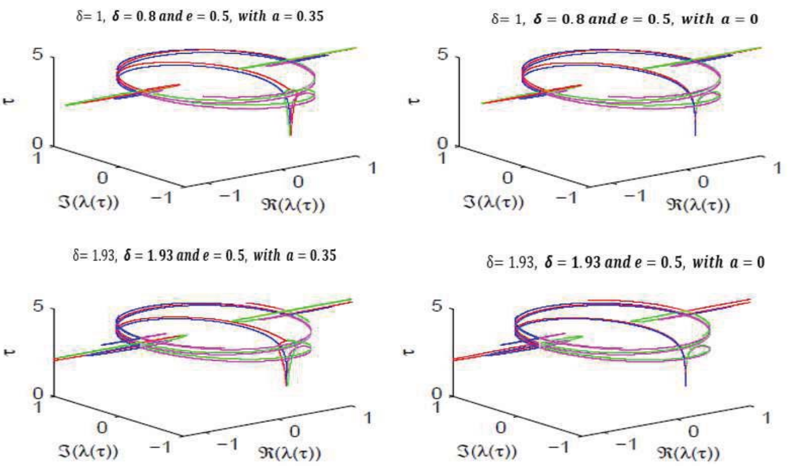

Figure 10. Spectral portrait of $\tau \mapsto \widetilde{X}_a(\tau, \delta, \epsilon, e)$ for $\tau \in [0, 2\pi]$ and $(\delta, \epsilon, e) \in \{(1, 0.8, 0.5), (1.93, 1.93, 0.5)\}$, with $a \in \{0; 0.35\}$

This Figure shows that of spectral portrait of $\widetilde{X}_a(\tau, \delta, \epsilon)$ does not change when the motion of the coupled pendulums is subjected to small rank-one perturbation or not.

In Figure 11, we notice that the unstable region is wider than the stable region when the motion of the coupled pendulum is subject to the effect of small rank-one perturbation. Because, $\|S^{(n_0)}(\tau)\|$ takes again much lager values when a is different to zero; and the region where $\delta_S(\tau)$ is represented in green color, is small when a is different to zero.

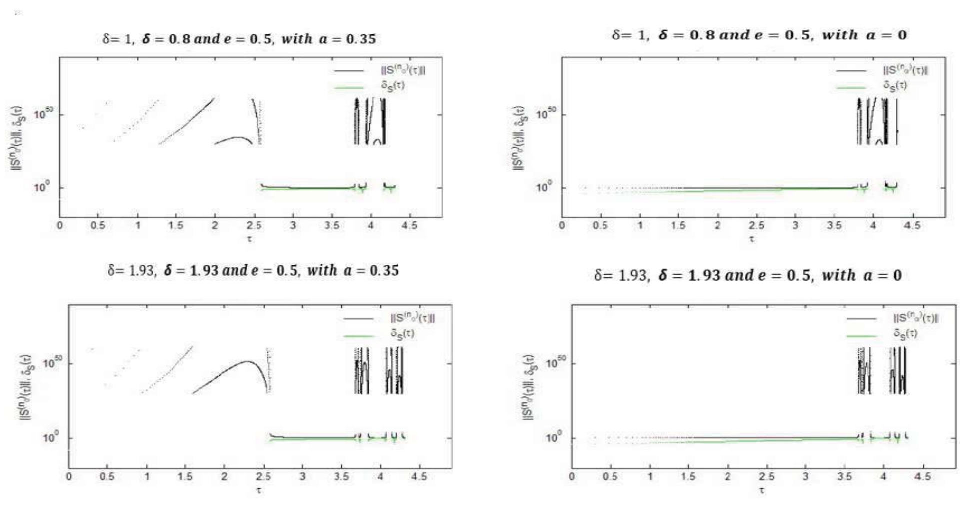

Figure 11. Graphs of $\tau \mapsto \|S^{(n_0)}(\tau)\|$ and $\tau \mapsto \|\delta_S(\tau)\|$ for $\tau \in [0, 2\pi]$ and $(\delta, \epsilon, e) \in \{(1, 0.8, 0.5), (1.93, 1.93, 0.5)\}$, with $a \in \{0; 0.35\}$

Figure 12 present the (strong) stability zone of $\widetilde{X}_a(2\pi, \delta, \epsilon,\ e)$. In this Figure, we observe that the unstable zone obtained, in presence of the rank-one perturbation is wider than that obtained in absence of this perturbation.

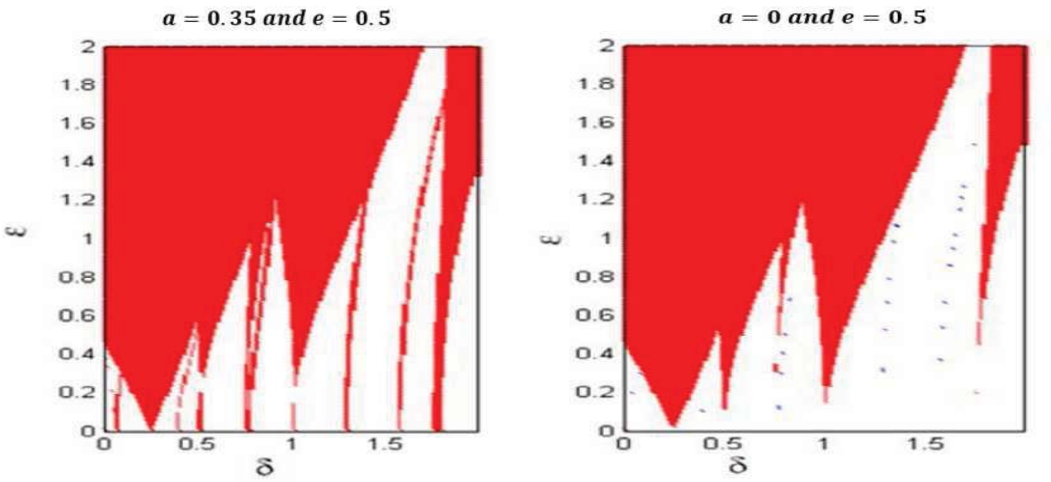

Figure 12. (Strong) stability zone of $\widetilde{X}_a(2\pi, \delta, \epsilon,\ e)$ for $(\delta, \epsilon) \in [0,\ 1.98] \times [0,\ 2]$, $a \in \{0; 0.35\}$ and $e = 0.5$

4. Triple Pendulum With Oscillating Supports

Here, we consider three identical simple pendulums attached to a common support (see Figures 13 and 17). In this problem, we restrict our study to the case where the support of each pendulum is subjected to an oscillating motion $f(t)$ defined by $f(t) = \alpha \cos(\Omega t)$ (see in (Hsu, 1961)).

4.1 Uncoupled Triple Pendulums With Oscillating Supports

In this first part, the three simple pendulums are uncoupled.

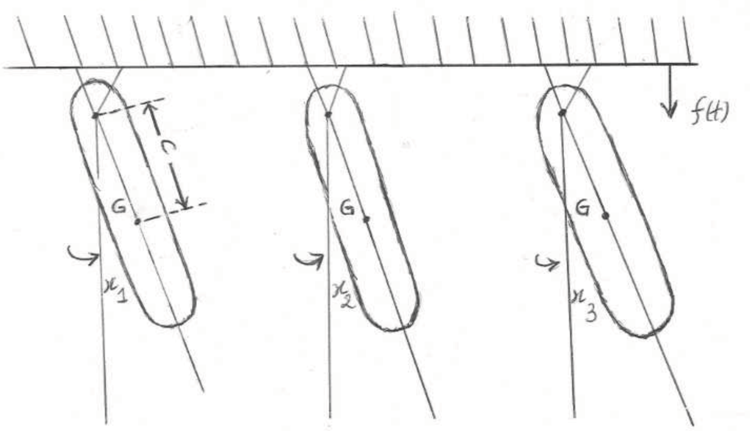

Figure 13. Model of the uncoupled triple pendulums with oscillating supports

Since the three pendulums are identical, according to (Hsu, 1961), the differential equation of motion will be the same for all three. Then, the equation of motion becomes:

$$\frac{d^2 x_i}{dt^2} + \frac{cg}{k_0^2}\left(1 - \frac{1}{g}\frac{d^2 f}{dt^2}\right) x_i = 0,\ i = 1, 2, 3; \tag{17}$$

where k_0 and c are defined in section 2.

Using the fact that $f(t) = \alpha\cos(\Omega t)$, the above differential system can be written as

$$\frac{d^2x_i}{dt^2} + \frac{cg}{k_0^2}\left(1 + \frac{\alpha\Omega^2}{g}\cos(\Omega t)\right)x_i = 0,\ i = 1, 2, 3; \tag{18}$$

According to (Hsu, 1961), using the change of variables $\tau = \Omega t$, the differential equation of motion of the triple pendulums may be reduced to:

$$\frac{d^2x_i}{d\tau^2} + (\delta + \epsilon\cos(\tau))\,x_i = 0,\ i = 1, 2, 3; \tag{19}$$

where

$$\epsilon = \frac{c\alpha}{k_0^2} \text{ and } \delta = \frac{cg}{k_0^2\Omega^2}$$

Introducing the change of variables given in (2) with $N = 3$, it is easy to see that the motion of the uncoupled system is gouverned by (1), with

$$H(\tau,\ \delta,\ \epsilon) = \begin{pmatrix} P(\tau,\ \delta,\ \epsilon) & 0_3 \\ 0_3 & I_3 \end{pmatrix},\ P(\tau,\ \delta,\ \epsilon) = ((\alpha_i(\tau))_{1\le i\le 3}) \text{ and } J = \begin{pmatrix} 0_3 & -I_3 \\ I_3 & 0_3 \end{pmatrix}.$$

To study the (strong) stability of the motion of the triple pendulums, we perturb the motion of the uncoupled system by the following rank-one matrix:

$$E_a(\tau, \delta,\ \epsilon) = u_a u_a^T J X(\tau, \delta,\ \epsilon) \tag{20}$$

where

$$u_a = a\begin{pmatrix} 1 \\ 0 \\ 0 \\ 0 \\ 0 \\ 0 \end{pmatrix} \text{ and } a \in [0,\ 1[.$$

From the above, we deduce that $\widetilde{X}_a(\tau, \delta,\ \epsilon)$ can be rewritten as:

$$\widetilde{X}_a(\tau, \delta,\ \epsilon) = \left(I + u_a u_a^T J\right) X(\tau, \delta,\ \epsilon)$$

and the equation of motion then becomes (see (Dosso, Arouna, & Koua Brou, 2018))

$$\left\{\begin{array}{rcl} J\dfrac{d\widetilde{X}_a(\tau, \delta,\ \epsilon)}{d\tau} & = & \underbrace{(I - u_a u_a^T J)^T H(\tau, \delta,\ \epsilon)(I - u_a u_a^T J)}_{\widetilde{H}(\tau,\delta,\ \epsilon,a)}\widetilde{X}_a(\tau, \delta,\ \epsilon), \\ \\ \widetilde{X}_a(0, \delta,\ \epsilon) & = & I + u_a u_a^T J \end{array}\right. \tag{21}$$

Figures 14 and 15 show respectively the spectral portrait of $\widetilde{X}_a(\tau, \delta, \epsilon)$ and the (strong) stability region of $\widetilde{X}_a(\tau, \delta, \epsilon)$ for $\tau \in [0, 2\pi]$ and $(\delta, \epsilon) \in \{(1, 0.8), (1.93, 1.93)\}$, with $a \in \{0, 0.35\}$.

In Figure 14, we note that the spectral portrait undergoes a slight modification in presence of the rank-one perturbation.

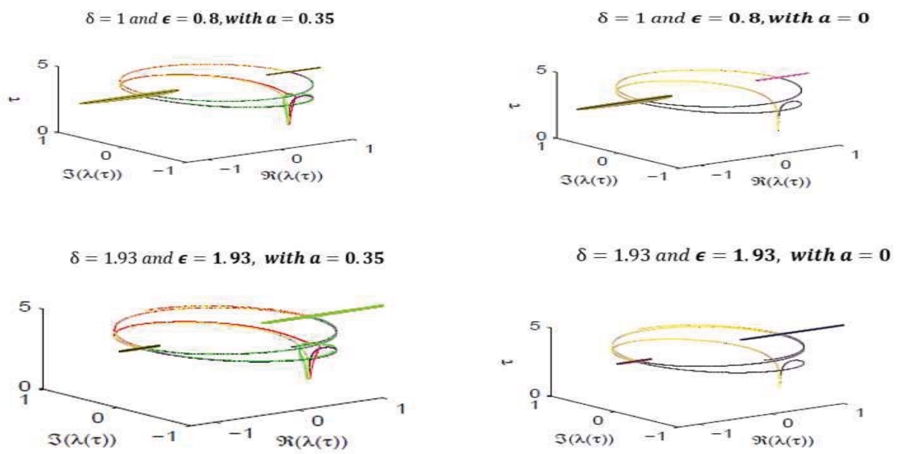

Figure 14. Spectral portrait of $\tau \mapsto \widetilde{X}_a(\tau, \delta, \epsilon)$ for $\tau \in [0, 2\pi]$ and $(\delta, \epsilon) \in \{(1, 0.8), (1.93, 1.93)\}$, with $a \in \{0, 0.35\}$

In figure 15, we observe that in presence of the rank-one perturbation there is a coarse widening of the unstable region and a narrowing of the stable region. Since, $\|S^{(n_0)}(\tau)\|$ takes much lager values when a is different to zero ; and the region where $\delta_S(\tau)$ is represented in green color, is small when a is different to zero.

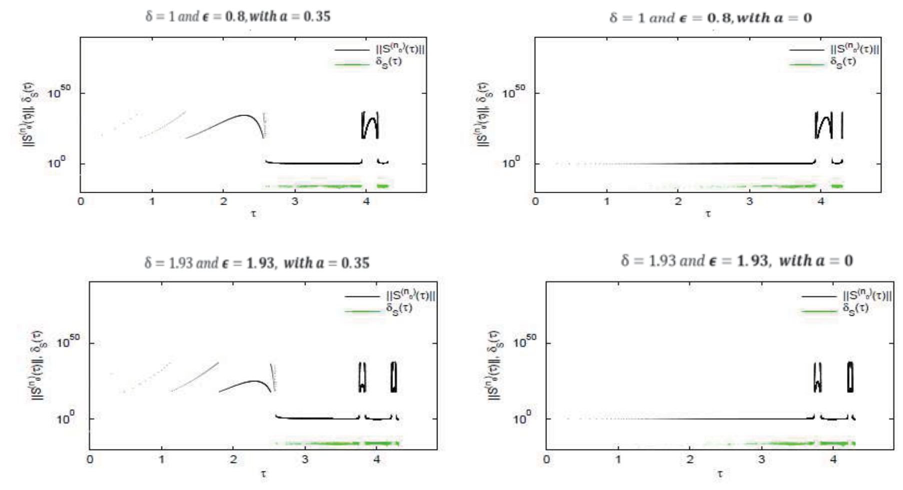

Figure 15. Graph of $\tau \mapsto \|S^{(n_0)}(\tau)\|$ and $\tau \mapsto \delta_S(\tau)$ for $\tau \in [0, 2\pi]$ and $(\delta, \epsilon) \in \{(1, 0.8), (1.93, 1.93)\}$, with $a \in \{0, 0.35\}$

In figure 16, the results obtained are consistent with the observations made in figure 8 of the second problem of this paper.

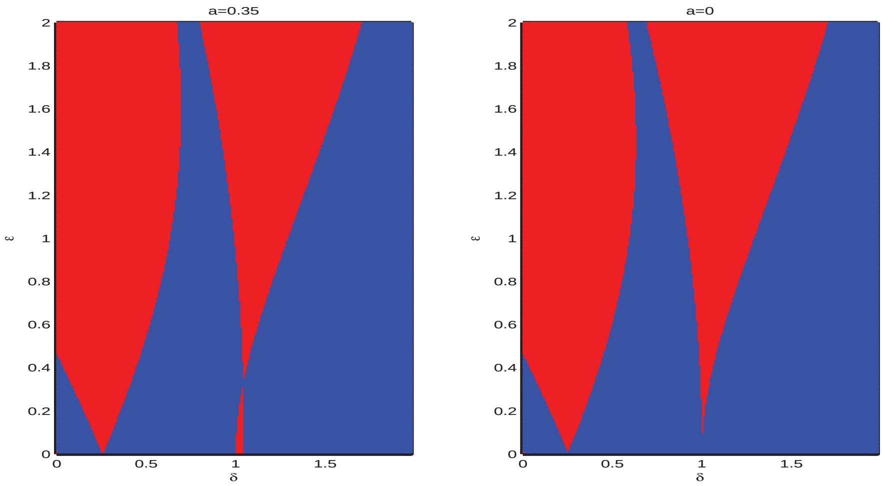

Figure 16. (Strong) stability zone of $\widetilde{X}_a(2\pi, \delta, \epsilon)$ for $(\delta, \epsilon) \in [0,\ 1.98] \times [0,\ 2]$ and $a \in \{0,\ 0.35\}$

4.2 Coupled Triple Pendulums With Oscillating Supports

In this part, we couple the three simple pendulums by two springs of identical constant of stiffness k.

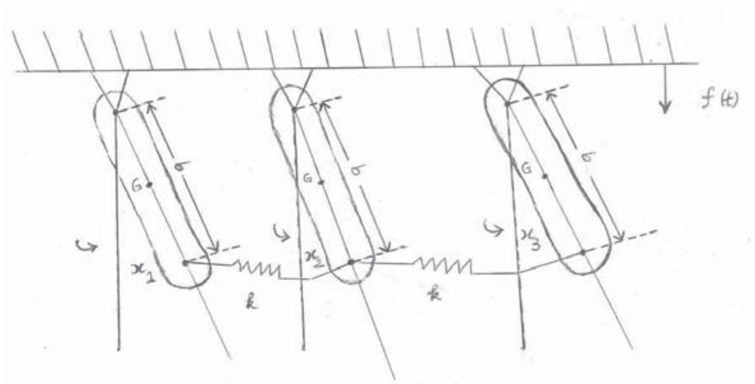

Figure 17. Model of coupled triple pendulum with oscillating supports

Before going on the purpose of this subsection, first we will search the equation of motion of the coupled triple pendulums. We know that the kinetic energy of each pendulum is of the form (see in (Timoshenko, Young, & Weaver, 1974)):

$$T_i = \frac{1}{2}m(\frac{k_0^2}{c})^2 \dot{x}_i^2,\ i = 1, 2, 3.$$

From a result of (Timoshenko, Young, & Weaver, 1974), we obtain the total kinetic energy of the coupled system by:

$$T = T_1 + T_2 + T_3 = \frac{1}{2}m(\frac{k_0^2}{c})^2 \left(\dot{x}_1^2 + \dot{x}_2^2 + \dot{x}_3^2\right).$$

Since the gravitational potential energy of each pendulum is given by:

$$U_i = \frac{1}{2}m\frac{k_0^2}{c}\left(g - \frac{d^2 f}{dt^2}\right)x_i^2,\ i = 1, 2, 3.$$

The total gravitational potential energy of the coupled system is given by:

$$U_{grav} = U_1 + U_2 + U_3 = \frac{1}{2}m\frac{k_0^2}{c}\left(g - \frac{d^2 f}{dt^2}\right)\left(x_1^2 + x_2^2 + x_3^2\right).$$

Since the elongation of the first spring (on the left) is given by $\frac{bk_0}{c}(x_2 - x_1)$ and that of the second spring (on the right) is given by $\frac{bk_0}{c}(x_3 - x_2)$, the potential energy of the spring is given by:

$$U_{ress} = \frac{1}{2}k(\frac{bk_0}{c})^2\left[(x_2 - x_1)^2 + (x_3 - x_2)^2\right] = \frac{1}{2}k(\frac{bk_0}{c})^2\left(x_1^2 + 2x_2^2 + x_3^2 - 2x_1x_2 - 2x_2x_3\right).$$

The total potential energy of the coupled double system is then given by:

$$U = U_{grav} + U_{ress} = \frac{1}{2}m\frac{k_0^2}{c}\left(g - \frac{d^2f}{dt^2}\right)\left(x_1^2 + x_2^2 + x_3^2\right) + \frac{1}{2}k(\frac{bk_0}{c})^2\left(x_1^2 + 2x_2^2 + x_3^2 - 2x_1x_2 - 2x_2x_3\right).$$

The Lagrangian is given by:

$$\begin{aligned}\mathcal{L} =& T - U\\ =& \frac{1}{2}m(\frac{k_0^2}{c})^2\left(\dot{x}_1^2 + \dot{x}_2^2 + \dot{x}_3^2\right) - \frac{1}{2}m\frac{k_0^2}{c}\left(g - \frac{d^2f}{dt^2}\right)\left(x_1^2 + x_2^2 + x_3^2\right) - \frac{1}{2}k(\frac{bk_0}{c})^2\left(x_1^2 + 2x_2^2 + x_3^2 - 2x_1x_2 - 2x_2x_3\right).\end{aligned}$$

The Lagrange's equations give:

$$\begin{cases}\frac{\partial\mathcal{L}}{\partial x_1} &=& \frac{d}{dt}\frac{\partial\mathcal{L}}{\partial\dot{x}_1}\\ \frac{\partial\mathcal{L}}{\partial x_2} &=& \frac{d}{dt}\frac{\partial\mathcal{L}}{\partial\dot{x}_2}\\ \frac{\partial\mathcal{L}}{\partial x_3} &=& \frac{d}{dt}\frac{\partial\mathcal{L}}{\partial\dot{x}_3}\end{cases}$$

$$\Longrightarrow\begin{cases}-m\frac{k_0^2}{c}\left(g - \frac{d^2f}{dt^2}\right)x_1 - k(\frac{bk_0}{c})^2x_1 + k(\frac{bk_0}{c})^2x_2 &=& m(\frac{k_0^2}{c})^2\ddot{x}_1\\ -m\frac{k_0^2}{c}\left(g - \frac{d^2f}{dt^2}\right)x_2 - 2k(\frac{bk_0}{c})^2x_2 + k(\frac{bk_0}{c})^2x_1 + k(\frac{bk_0}{c})^2x_3 &=& m(\frac{k_0^2}{c})^2\ddot{x}_2\\ -m\frac{k_0^2}{c}\left(g - \frac{d^2f}{dt^2}\right)x_3 - k(\frac{bk_0}{c})^2x_3 + k(\frac{bk_0}{c})^2x_2 &=& m(\frac{k_0^2}{c})^2\ddot{x}_3\end{cases}$$

$$\Longrightarrow\begin{cases}\ddot{x}_1 + \left(\frac{cg}{k_0^2} + \frac{kb^2}{mk_0^2} - \frac{c}{k_0^2}\frac{d^2f}{dt^2}\right)x_1 - \frac{kb^2}{mk_0^2}x_2 &=& 0\\ \ddot{x}_2 + \left(\frac{cg}{k_0^2} + \frac{2kb^2}{mk_0^2} - \frac{c}{k_0^2}\frac{d^2f}{dt^2}\right)x_2 - \frac{kb^2}{mk_0^2}x_1 - \frac{kb^2}{mk_0^2}x_3 &=& 0\\ \ddot{x}_2 + \left(\frac{cg}{k_0^2} + \frac{kb^2}{mk_0^2} - \frac{c}{k_0^2}\frac{d^2f}{dt^2}\right)x_3 - \frac{kb^2}{mk_0^2}x_2 &=& 0\end{cases} \tag{22}$$

which implies that the motion of the triple pendulums can be governed by the following differential system:

$$\frac{d^2x}{dt^2} + \left(B_0 - \frac{c}{k_0^2}\frac{d^2f}{dt^2}I_3\right)x = 0, \tag{23}$$

where

$$x = \begin{pmatrix} x_1\\ x_2\\ x_3\end{pmatrix}, \text{ and } B_0 = \begin{pmatrix}\frac{cg}{k_0^2} + \frac{kb^2}{mk_0^2} & -\frac{kb^2}{mk_0^2} & 0\\ -\frac{kb^2}{mk_0^2} & \frac{cg}{k_0^2} + \frac{2kb^2}{mk_0^2} & -\frac{kb^2}{mk_0^2}\\ 0 & -\frac{kb^2}{mk_0^2} & \frac{cg}{k_0^2} + \frac{kb^2}{mk_0^2}\end{pmatrix},$$

with m the mass of each pendulum and b the distance from the point of suspension to the point where the coupling spring is attached.

Replacing $f(t)$ by its new expression in equation (23), we get the following equation

$$\frac{d^2x}{dt^2} + \left(B_0 + \frac{c\alpha\Omega^2}{k_0^2}\cos(\Omega t)I_3\right)x = 0 \tag{24}$$

Using the change of variable $\tau = \Omega t$, the equation of the triple pendulums motion then becomes:

$$\frac{d^2x}{d\tau^2} + (B_1 + \epsilon\cos(\tau)I_3)\,x = 0 \tag{25}$$

where

$$x = \begin{pmatrix} x_1 \\ x_2 \\ x_3 \end{pmatrix},\ B_1 = \begin{pmatrix} \delta+e & -e & 0 \\ -e & \delta+2e & -e \\ 0 & -e & \delta+2e \end{pmatrix},\ \text{with } \delta = \frac{cg}{\Omega^2k_0^2},\ e = \frac{kb^2}{mk_0^2\Omega^2} \text{ and } \epsilon = \frac{c\alpha}{k_0^2}.$$

With the change of variable given in (2), we get system (1) with

$$H(\tau,\ \delta,\ \epsilon,\ e) = \begin{pmatrix} P(\tau,\ \delta,\ \epsilon,\ e) & 0_3 \\ 0_3 & I_3 \end{pmatrix},$$

and

$$P(\tau,\ \delta,\ \epsilon,\ e) = \begin{pmatrix} \delta+e+\epsilon\cos(\tau) & -e & 0 \\ -e & \delta+2e+\epsilon\cos(\tau) & -e \\ 0 & -e & \delta+e+\epsilon\cos(\tau) \end{pmatrix}.$$

In this part, we assume that the motion of the coupled system is perturbed by a matrix of rank one of the form (16), where

$$u_a = a\begin{pmatrix} 1 \\ 0 \\ 0 \\ 0 \\ 0 \\ 0 \end{pmatrix} \text{ and } a \in [0,\ 1[.$$

Then according to (Dosso, Arouna, & Koua Brou, 2018), it is easy to see that the equation of the motion of the coupled system is governed by equation (21).

In Figures 18 and 19, numerical simulations were done with

$$\tau \in [0,\ 2\pi],\ (\delta,\ \epsilon,\ e) \in \{(1, 0.8, 0.5),\ (1.93,\ 1.93,\ 0.5)\} \text{ and } a \in \{0,\ 0.35\}.$$

As expected, we can visualize respectively, the spectral portrait of $\widetilde{X}_a(\tau, \delta, \epsilon, e)$ and the (strong) stability zone of the motion of the system. In Figure 18, we observe small change in the spectral portrait of $\widetilde{X}_a(\tau, \delta, \epsilon, e)$.

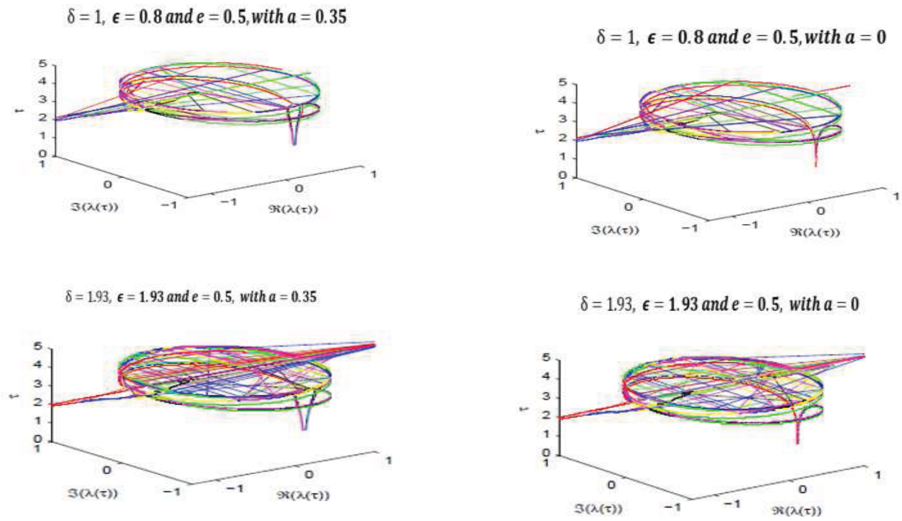

Figure 18. Spectral portrait of $\tau \mapsto \widetilde{X}_a(\tau,\ \delta,\ \epsilon,\ e)$ for $\tau \in [0,\ 2\pi]$ and $(\delta,\ \epsilon,\ e) \in \{(1, 0.8, 0.5),\ (1.93,\ 1.93,\ 0.5)\}$, with $a \in \{0,\ 0.35\}$

In figure 19, we note that in presence of the rank-one perturbation, the motion of the coupled system becomes very unstable. Because, the euclidian norm of $S^{(n_0)}(\tau)$ takes much lager values when a is different to zero; and the region where $\delta_S(\tau)$ is represented in green color, is small when a is different to zero.

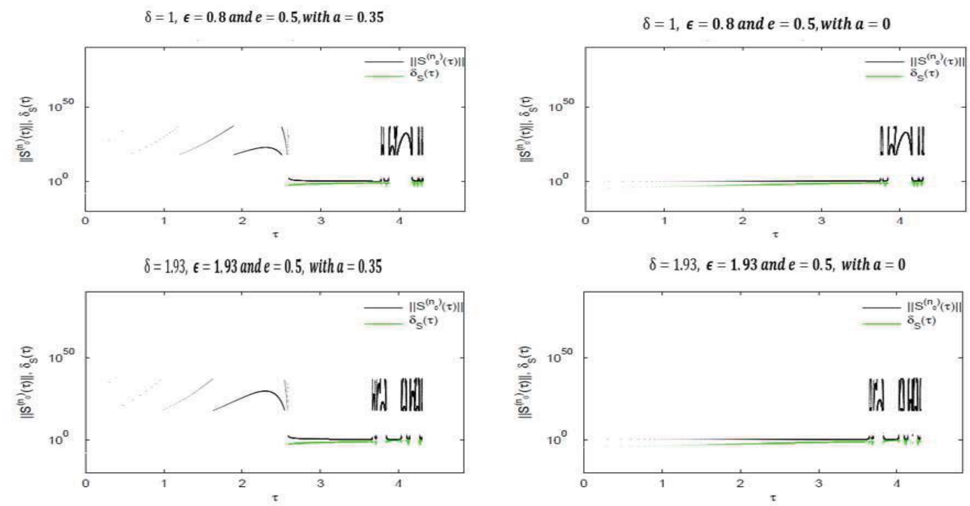

Figure 19. Graph of $\tau \mapsto \|S^{(n_0)}(\tau)\|$ and $\tau \mapsto \delta_S(\tau)$ for $\tau \in [0,\ 2\pi]$ and $(\delta,\ \epsilon,\ e) \in \{(1, 0.8, 0.5),\ (1.93,\ 1.93,\ 0.5)\}$, with $a \in \{0,\ 0.35\}$

In Figure 20, we note a slight difference between the two figures due to the small rank-one perturbation of the system described by our triple coupled pendulums.

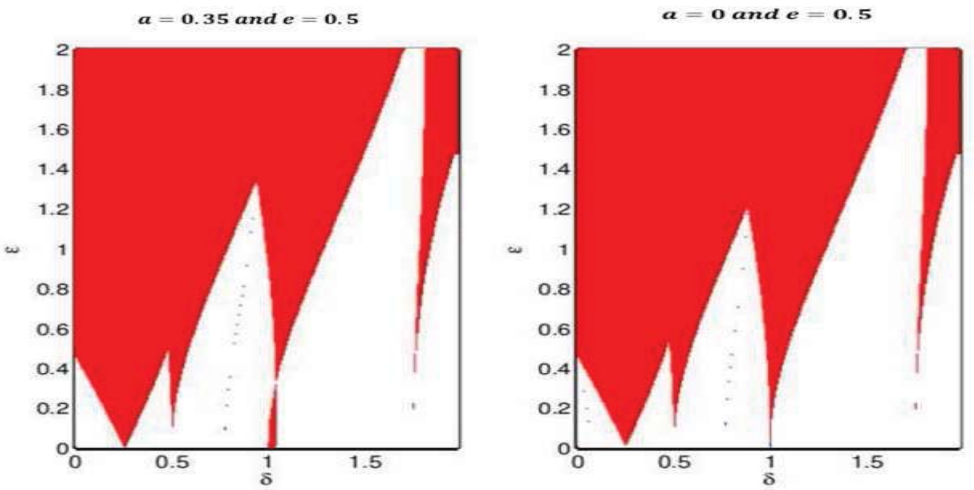

Figure 20. (Strong) stability zone of $\widetilde{X}_a(2\pi,\ \delta,\ \epsilon,\ e)$ for $(\delta, \epsilon) \in [0,\ 1.98] \times [0,\ 2]$, $a \in \{0, 0.35\}$ and $e = 0.5$

5. Double Pendulum With Fixed Support

We consider a double pendulum made up of two points masses m_1 and m_2 with an absolutely rigid end of length l_1 and the other elastic of stiffness coefficient c and static elongation λ. These two ends are linked between them in m_1, and the end of the first pendulum is linked to its other end O, considered as the origin of the coordinate system $\left(O,\ \overrightarrow{i},\ \overrightarrow{j}\right)$ (see Figure below). The connections and the oscillations of the double pendulum are supposed respectively perfect and weak.

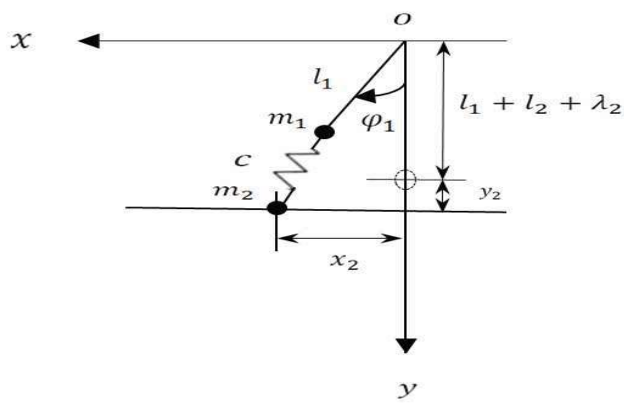

Figure 21. Double pendulum model with fixed support

According to (Yakubovich & Starzhinskii, 1975), the equation of the pendulum movement is given by:

$$\frac{d^2y}{d\tau^2} + P(\tau,\ \epsilon,\ \delta)y = 0, \tag{26}$$

where

$$y = \begin{pmatrix} \phi \\ \xi \end{pmatrix}$$

and

$$P(\tau,\ \epsilon,\ \delta) = \begin{pmatrix} k\delta\,(1+\nu) + \nu k\epsilon\cos(\tau) + \nu\dfrac{\delta+\epsilon\cos\tau}{1+\delta+\epsilon\cos\tau} & -\sqrt{\nu}\dfrac{\delta+\epsilon\cos\tau}{1+\delta+\epsilon\cos\tau} \\ -\sqrt{\nu}\dfrac{\delta+\epsilon\cos\tau}{1+\delta+\epsilon\cos\tau} & \dfrac{\delta+\epsilon\cos\tau}{1+\delta+\epsilon\cos\tau} \end{pmatrix},$$

with

$$\tau = \Omega t,\ \xi = \sqrt{\nu}\frac{x_2}{l_1},\ \nu = \frac{m_2}{m_1},\ k = \frac{l_2}{l_1},\ \delta = \frac{\lambda_2}{l_2} \text{ and } \epsilon = \frac{Y_2}{l_2}.$$

Using the change of variables (2) with $N = 2$, we obtain the Hamiltonian system with 2π-periodic coefficients (1) with :

$$H(t) = \begin{pmatrix} P(\tau,\ \epsilon\ \delta) & 0_2 \\ 0_2 & I_2 \end{pmatrix} \text{ and } J = \begin{pmatrix} 0_2 & -I_2 \\ I_2 & 0_2 \end{pmatrix}.$$

To simplify the problem, we take: $m_1 = 2g,\ m_2 = 5g,\ l_1 = 0.5m,\ l_2 = 1m,$ and $\Omega = 1$; and we subject the motion of the system to a rank-one perturbation of the form (11). Then, the equation of the movement of the system can be put in the form (13). To study the (strong) stability of the motion of the pendulum for $\tau \in [0,\ 2\pi]$, numerical simulations were done with $(\epsilon,\delta) \in \{(0.05, 0.5), (0.2,\ 0.6)\}$ and $a = 0,\ 0.35$.

In Figure 22, we present the spectral portrait of $\widetilde{X}_a(\tau,\epsilon,\delta)$. This Figure shows that the spectral portrait does not changes in presence or in absence of the rank-one perturbation.

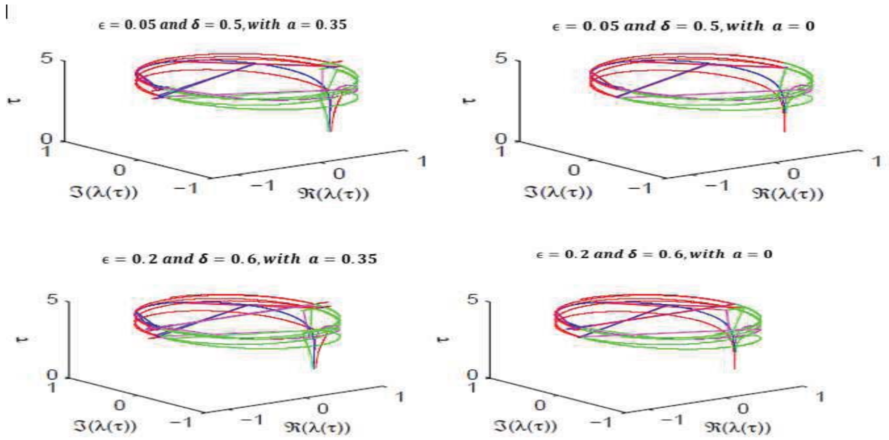

Figure 22. Spectral portrait of $\tau \mapsto \widetilde{X}_a(\tau,\epsilon,\delta)$ for $\tau \in [0,\ 2\pi]$ and $(\epsilon,\delta) \in \{(0.05, 0.5),\ (0.2,\ 0.6)\}$, with $a = 0, 0.35$

Figure 23 shows the (strong) stability zone of $\widetilde{X}_a(\tau, \epsilon, \delta)$ for $\tau \in [0,\ 2\pi]$ and $(\epsilon, \delta) \in \{(0.05, 0.5),\ (0.2,\ 0.6)\}$, with $a = 0, 0.35$. In this zones, we note that the presence of rank-one perturbation is a factor that increase the loss of (strong) stability of the motion of the pendulum. In fact, the euclidian norm of $S^{(n_0)}(\tau)$ takes much lager values when a is different to zero ; and the region where $\delta_S(\tau)$ is represented in green color, is small when a is different to zero.

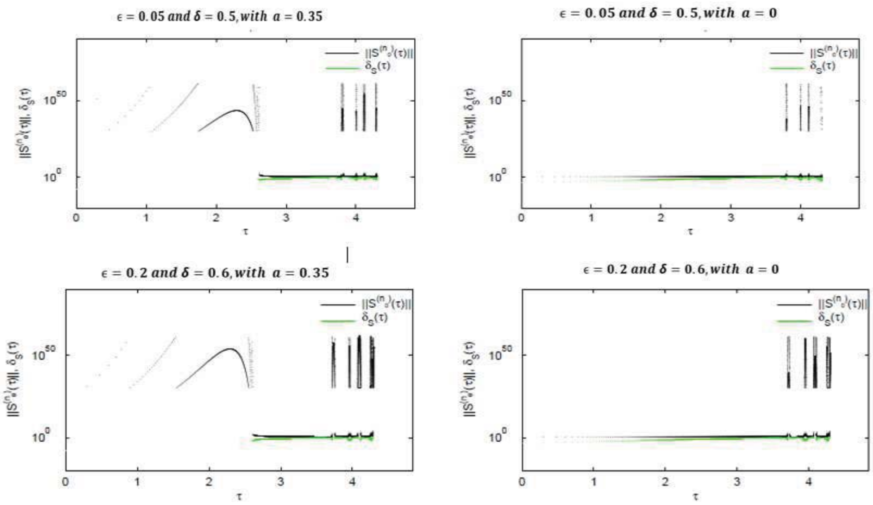

Figure 23. Graphs of $\tau \mapsto \|S^{(n_0)}(\tau)\|$ and $\tau \mapsto \delta_S(\tau)$ for $\tau \in [0,\ 2\pi]$ and $(\epsilon, \delta) \in \{(0.05, 0.5),\ (0.2,\ 0.6)\}$, with $a = 0, 0.35$

In the (strong) stability zone of the double pendulum(see Figure 24), we can note a small different between the two figures due to the presence of the rank-one perturbation.

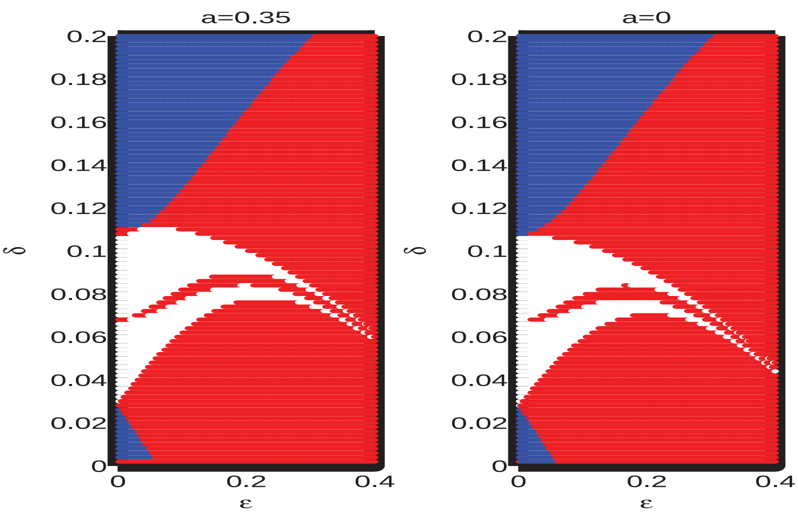

Figure 24. (Strong) stability zone of $\widetilde{X}_a(2\pi,\ \epsilon,\ \delta)$ for $(\epsilon,\ \delta) \in [0,\ 0.8] \times [0,\ 0.2]$ and $a = 0,\ 0.35$

6. Concluding Remark

In this article, we have applied the theory of rank-one perturbation introduced in (Dosso, Arouna, & Koua Brou, 2018) to some problems governed by pendulum systems. The systems concerned are the pendulum with oscillating supports and double pendulum with fixed supports. To do this work, firstly, we rewrite the motion of these systems in Hamiltonian form (1). Secondly, we contented ourselves with a study of (strong) stability introduced in (Dosso, 2006) to analyze the effect of the rank-one perturbation on the motion of these pendulum systems. The results obtained show that the presence of the perturbation on the motion of the pendulum system favors more the loss (strong) stability of the motion of systems.

Acknowledgments

We express our sincere thanks to the anonymous reviewer for his careful reading of the paper and his valuable suggestions to improve the quality of the paper.

References

Arouna, T. G. Y., & Dosso, M. (2018). A structured approach to a perturbation of Hamiltonian systems with periodic coefficients. *International Journal of Recent Scientific Research, 9,* 25846-25856. http://dx.doi.org/10.24327/ijrsr.2018.0904.1941

Arouna, T. G. Y., Dosso, M., & Koua Brou, J. C. (2018). On a pertubation theory of Hamiltonian systems with periodic coefficients. *International Journal of Numerical Methods and Applications, 17*, 47-89. http://dx.doi.org/10.17654/NM017020047

Dosso, M. (2006). *Sur quelques algorithms d'analyse de stabilité forte de matrices symplectiques*. PHD Thesis, Université de Bretagne Occidentale. Ecole Doctorale SMIS, Laboratoire de Mathématiques, UFR Sciences et Techniques. https://tel.archives-ouvertes.fr/tel-00626273

Dosso, M., Arouna, T. G. Y., & Koua Brou, J. C. (2019). Rank-k perturbation of Hamiltonian systems with periodic coefficients and applications. *European Journal of Pure and Applied Mathematics, 12*, 1744-1770. https://doi.org/10.29020/nybg.ejpam.v12i4.3574

Dosso, M., Arouna, T. G. Y., & Koua Brou, J. C. (2018). On rank one perturbation of Hamiltonian system with periodic coefficients. *Wseas Translations on Mathematics, 17*, 377-384. Retrieved from https://www.wseas.org/multimedia/journals/mathematics/2018/a885806-897.pdf

Dosso, M., & Sadkane, M. (2013). On the strong stability of symplectic matrices. *Numerical Linear Algebra with Applications, 20,* 234-249. https://doi.org/10.1002/nla.834

Dosso, M., & Coulibaly, N. (2014). Symplectic matrices and strong stability of Hamiltonian systems with periodic coefficients. *Journal of Mathematical Sciences : Advances and Applications, 28*, 15-38. http://scientificadvances.co.in/abstract/1/139/823

Godunov, S. K., & Sadkane, M. (2001). Numerical determination of a canonical form of a symplectic matrix. *Siberian Mathematical Journal, 42,* 629-647. https://doi.org/10.1023/A:1010485128908

Godunov, S. K., & Sadkane, M. (2006). Spectral analysis of symplectic matrices with application to the theory of parametric resonance. *SIAM Journal on Matrix Analysis and Applications, 28,* 1083-1096. https://doi.org/10.1137/040618503

Hoffmann, E., & Stroobant, V. (2007) *Mass spectrometry. Principles and applications* (3rd ed.). ISBN 13: 9780470512135

Hsu, C. S. (1961). On a Restricted Class of Coupled Hill's Equations and Some Applications. *Journal of Applied Mechanics, 28*, 551-556. https://doi.org/10.1115/1.3641781

Lalanne, M., Berthier, P., & Der Hagopian, J. (1984) *Mechanical vibrations for engineers*, Chichester, Wiley Interscience. ISBN 13: 9780471901976

Mathieu, E. (1868). Mémoire sur le mouvement vibratoire d'une membrane de forme elliptique. *Journal des Mathmatiques Pures et Appliques, 13*, 137-203. http://eudml.org/doc/234720

Timoshenko, S. P., Young, D. H., & Weaver, W. (1974) *Vibrations problems in engineering*. John Wiley and Sons. ISBN 13: 9780471632283.

Yakubovich, V. A., & Starzhinskii, V. M. (1975) *Linear differential equqtions with periodic coefficients*, Wiley, New York. ISBN 10: 0706514807